Published in final edited form as:
Arch Oral Biol. 2009 December ; 54(12): 1091–1098. doi:10.1016/j.archoralbio.2009.10.001.

Analysis of Microarchitectural Changes in a Mouse Temporomandibular Joint Osteoarthritis Model

J. Chen, DDS PhD[*,1], **T. Gupta, DMD**[1], **J.A. Barasz, MS**[1], **Z. Kalajzic, MD**[1], **W-C. Yeh, DDS MS**[1], **H. Drissi, PhD**[2], **A.R. Hand, DDS**[1], and **S. Wadhwa, DDS PhD**[1]

[1]University of Connecticut Health Center, School of Dental Medicine, Department of Craniofacial Sciences, Farmington, CT 06030

[2]University of Connecticut Health Center, New England Musculoskeletal Institute Department of Orthopedics, Farmington, CT 06030

Abstract

Objective—Little is known about the natural progression of the disease process of temporomandibular joint (TMJ) osteoarthritis (OA), which affects approximately 1 % of the US population. The goal of this study was to examine the early microarchitectural and molecular changes in the condylar cartilage and subchondral bone in *biglycan/fibromodulin (Bgn/Fmod)* double-deficient mice, which develop TMJ-OA at 6 months.

Methods—TMJs from 3 month old (n=44) and 9 month old (n=52) wild-type (WT n=46) and *Bgn/Fmod* (n=50) double-deficient mice were evaluated. Micro-CT analysis of the subchondral bone (n=24), transmission electron microscopy for condylar cartilage fibril diameters (n=26), and real time PCR analysis for gene expression for bone and cartilage maturation markers (n=45) was performed.

Results—A statistically significant increase in collagen fibril diameter of the condylar cartilage and a decrease in expression of *Parathyroid related protein* in the mandibular condylar head were observed in the 3 month *Bgn/Fmod* double-deficient mice compared to WT controls. The 9 month *Bgn/Fmod* double-deficient mouse demonstrated an increase in bone volume and total volume in subchondral bone, and an increase in the expression of *Collagen Type X* and *Aggrecan* in the mandibular condylar head compared to the WT controls.

Conclusion—We found that **c**hanges in the microarchitecture of the condylar cartilage preceded changes in the subchondral bone during OA in the TMJ in *Bgn/Fmod* double-deficient mice.

INTRODUCTION

The National Institute of Dental and Craniofacial Research of the National Institutes of Health reported that temporomandibular joint (TMJ) disease is the second most common musculoskeletal disease in the United States, with 10.8 million people suffering from TMJ problems at any given time. The TMJ is different than other joints in a number of ways (1).

***Corresponding Author:** Dr. Sunil Wadhwa Division of Orthodontics Department of Craniofacial Sciences School of Dental Medicine UCHC, Farmington CT 06030 860-679-4899; 860-679-1920 (fax) Wadhwa@uchc.edu.
*Co First authors

Some of these differences are that the TMJ is composed of fibrocartilage instead of hyaline cartilage (2) and the mandibular condylar cartilage undergoes endochondral ossification during the active growth period (3). One form of TMJ disease is osteoarthritis (OA) (4). While imaging techniques are used to diagnose TMJ-OA, such diagnosis can only be made after the TMJ has been subjected to irreversible damage. Therefore, very little is known about the early stages of the disease process. With only a limited capacity for TMJ regeneration, greater understanding of the molecular and microarchitectural structural changes in the early stages of TMJ-OA is critical. Such research has been facilitated by the use of animal models to study the entire TMJ-OA disease process (5).

Several animal models have been developed to study the effects of TMJ-OA. One such TMJ-OA model that covers the whole diseases process is the biglycan and fibromodulin (*Bgn/Fmod*) double-deficient mouse model. BGN and FMOD are members of the small leucine-rich protein family (6) essential in extracellular matrix organization in bone (7), cartilage (8), and tendons (9,10). *Bgn/Fmod* double-deficient mice develop OA in a number of joints (10), including the TMJ (5). The *Bgn/Fmod* double-deficient mice also develop knee OA at 2 months, and by 5 months almost complete destruction of the joint occurs (11). In this joint, structural weaknesses of tendons are thought to be the origin of OA (10). In addition, other studies have shown that knee OA is associated with the articular chondrocytes undergoing endochondral ossification inappropriately (12). In contrast, TMJ-OA is first detected at 6 months in the *Bgn/Fmod* double-deficient mice, and the disease progresses gradually with age (5). In addition, both the origin of OA in the TMJ as well as whether reactivation of endochondral maturation during TMJ-OA occurs in the *Bgn/Fmod* double deficient mice are unknown. Therefore, the goals of this study were to examine chondrocyte maturation markers and microarchitectural changes within the TMJ during early and active TMJ-OA. Greater understanding of such changes occurring in TMJ-OA samples is critical in the future development of treatment modalities that prevent or reverse the disease process.

MATERIALS & METHODS

Mice

All experiments were performed under an institutionally approved protocol for the use of animals in research (University of Connecticut Health Center 2005-195). B6/129 WT mice were obtained from Jackson Laboratory (Bar Harbor, ME) and the double deficient *Bgn/Fmod* mice in the B6/129 background were obtained from Dr. Marian Young (National Institute of Dental and Craniofacial Research, Bethesda, MD) (10). Both male and female mice (n= 96) were used in this study. Mice were euthanized at 3 or 9 months of age.

Histology

For each genotype and age, heads from at least 3 animals were dissected in two halves. After removal of the brain, the specimens were fixed for 2 weeks at room temperature in 10% formalin. After being washed in tap water for 5 minutes, they were decalcified in 15% EDTA for 1 week.. Serial sections of the TMJ were then performed with every 5^{th} section stained with H&E or Safranin O (13).

Micro-CT

The three-dimensional morphometric analysis of the subchondral bone of the mandibular condylar head was evaluated using microcomputed tomography (micro-CT) (μCT 20, Scanco Medical AG, Bassersdorf, Switzerland). Mandibles from 3 month WT (n = 6), 3 month *Bgn/Fmod* double-deficient (n = 5), 9 month WT (n = 6), and 9 month *Bgn/Fmod* double-deficient (n = 7) mice were dissected and bisected at the level of the symphysis and stored in 70% ethanol.

Analysis of the mandibular condylar head included the bone surface, bone volume, total volume, trabecular number, trabecular thickness, and trabecular spacing.

Transmission Electron Microscopy

Mandibles were dissected from 3 month WT (n = 6), 3 month *Bgn/Fmod* double-deficient (n = 6), 9 month WT (n = 6), and 9 month *Bgn/Fmod* double-deficient (n = 8) mice. The mandibles were bisected and placed in 2.5 % glutaraldehyde/2.0 % paraformaldehyde, buffered to a pH 7.3 with 0.1 M sodium cacodylate. The hemi-mandibles were placed in the fixative within minutes of sacrifice. The fixation proceeded for 24 hr at 4 °C. The specimens were then removed from the fixative and placed in 4 % EDTA at 4 °C with constant stirring for 12 d (14). The condyles were removed from the hemimandibles and further demineralized for an additional 4 d, then rinsed in several changes of cold (4 °C) 0.1 M cacodylate buffer. Rinsed segments were postfixed with 1 % osmium tetroxide in cacodylate buffer at room temperature for 2 hr, dehydrated in a graded ethanol series and embedded in Polybed resin (Polysciences). The condyles were then sectioned sagittally at 1 μm and stained with methylene blue/Azure II for light microscopy. Thin sections, 70-90 nm, were cut with a diamond knife, collected on uncoated 200 mesh copper-rhodium grids, and stained sequentially with 1 % phosphotungstic acid, 6 % uranyl acetate in 50 % methanol, and Sato's lead citrate (15). The sections were examined and photographed in a Philips CM10 transmission electron microscope at 60 kV. A total of 27 mandibular condylar heads were examined. Ten micrographs of longitudinally oriented collagen fibrils from the middle third of the condylar cartilage were taken at a magnification of 52,000 X. The negatives were scanned at a resolution of 1200 pixels per inch in an Epson Perfection V750 Pro scanner. The images were imported into Adobe Photoshop CS2 (version 9.0.2) and levels and contrast were adjusted. Ten collagen fibrils per image for a total of one hundred collagen fibrils per condylar head were measured using Photoshop. A grid was constructed in Photoshop and ten collagen fibrils were chosen at random and their diameters measured using the measure tool. The examiner was blinded to the samples being measured.

RNA Extraction and PCR Amplification

The mandibular condyle was carefully isolated with the soft tissues removed using a dissecting microscope. Total RNA was obtained from the condylar head, which contained both condylar cartilage and subchondral bone, and extracted with TRIzol Reagent (Invitrogen Life Technologies, Carlsbad, CA) following the manufacturer's protocol. Total RNA obtained from the left and right TMJ of one mouse was pooled together. Total RNA was converted to cDNA by ABI High Capacity cDNA Archive Kit (Applied Biosystems, Foster City, CA) following the manufacturer's protocol. Real time PCR was performed for the expression of different genes in separate wells (singleplex assay) of 96-well plates in a reaction volume of 20 μl. *Gapdh* was used as an endogenous control. Three replicates of each sample were amplified using Assays-on-Demand Gene Expression for the particular gene of interest with predesigned unlabeled gene-specific PCR primers and TaqMan MGB FAM dye-labeled probe. The PCR reaction mixture (including 2 X TaqMan Universal PCR Master Mix, 20 X Assays-on-Demand Gene Expression Assay Mix, 50 ng of cDNA) was run in Applied Biosystems ABI Prism 7300 Sequence Detection System instrument utilizing universal thermal cycling parameters. For the genes for which the efficiencies of target and endogenous control amplification were approximately equal, relative expression in a test sample compared to a reference calibrator sample (ΔΔCt Method) was used for data analysis. For the genes that were not amplified with the same efficiency as the endogenous control, the Relative Standard Curve method, in which the target quantity was determined from the standard curve and divided by the target quantity of the calibrator, was used. Gene expression was performed for collagen I (*Col I*), parathyroid hormone related protein (*PTHrP*), SRY-box containing gene 9 (*Sox9*), collagen type II (*Col*

II), Indian hedgehog (*Ihh*), collagen type X (*Col X*), vascular endothelial growth factor (*Vegf*), osteopontin (*Opn*), and *Aggrecan*.

Statistical Analysis

Statistical significance of differences among means was determined by analysis of variance with post-hoc comparison of more than two means by the Bonferroni method or the Mann-Whitney rank sum test for nonparametric populations using SigmaStat (Jandel Scientific, San Rafael, CA).

RESULTS

TMJ sections from 3 and 9 month old WT and *Bgn/Fmod* double-deficient mice were stained with Safranin O. Safranin O is a cationic dye that binds to the negatively charged glycosaminoglycans. At 3 months, Safranin O staining extended more superiorly in the mandibular condylar cartilage from the *Bgn/Fmod* double-deficient mice compared to the WT mice. At 9 months of age, significant histological differences were observed between the WT and *Bgn/Fmod* double-deficient TMJs (Fig. 1). The 9 month *Bgn/Fmod* double-deficient TMJ contained large vertical clefts, and chondrocytes had begun to lose their regular columnar organization. The WT TMJs did not express either of these two characteristics.

Changes in Micro-architecture of the Subchondral Bone During TMJ-OA

TMJ-OA induced temporal changes in the microarchitecture of the mandibular condylar subchondral bone were evaluated by micro-CT analysis. No significant differences were identified in any of the micro-CT parameters examined between WT and *Bgn/Fmod* double-deficient mice at 3 months. However, at 9 months, a statistically significant decrease in trabecular thickness, and a statistically significant increase in trabecular spacing, trabecular number, total volume, bone volume, and bone surface were observed in the *Bgn/Fmod* double-deficient mice versus the WT controls (Fig. 2).

Transmission Electron Microscopy

TMJ-OA induced changes in collagen fibril diameter and organization of the mandibular condylar cartilage was evaluated using transmission electron microscopy (TEM) analysis. Measurements of collagen fibrils in the electron micrographs revealed a statistically significant increase in collagen fibril diameters in 3 month old *Bgn/Fmod* double-deficient mice versus the WT controls (Fig. 3). No statistically significant difference in collagen fibril diameters was observed between 9 month old WT and *Bgn/Fmod* double-deficient mice.

Gene Expression

Real time PCR gene expression analysis showed a statistically significant decrease in *PTHrP* in 3 month old *Bgn/Fmod* double-deficient mice compared to WT mice. A statistically significant increase in *Col X* and *Aggrecan* expression was found in 9 month *Bgn/Fmod* double-deficient mice compared to the WT controls (Fig. 4).

DISCUSSION

Bgn/Fmod double-deficient mice first develop TMJ-OA at 6 months. In this study, we examined the microarchitectural and molecular changes that occurred prior to onset of overt TMJ-OA at 3 months in the *Bgn/Fmod* double-deficient mice. BGN and FMOD are expressed in both the mandibular condylar cartilage (5) and in the bone (16). Previous studies have shown that male *Bgn* deficient mice have age related osteoporosis (17). *Fmod* deficient mice, on the other hand, develop knee osteoarthritis (18). In this study, we found a significant increase in

the collagen fibril diameters in the condylar cartilage and no differences in micro-CT parameters in the subchondral bone from 3 month *Bgn/Fmod* double-deficient mice compared to age matched WT controls. These results suggest that microarchitectural changes in the condylar cartilage preceded changes in the subchondral bone during TMJ-OA in the *Bgn/Fmod* double-deficient mice. Similar results of changes in the condylar cartilage preceding changes in the subchondral bone have been reported in other TMJ-OA animal models (19). In other joints, subchondral bone remodeling is thought to play a role in the progression of OA, (20,21) and in humans clinical trials therapies targeted at inhibiting subchondral bone resorption (bisphosphonates) have been successful in reducing the cartilage degradation (22) (23). In our model, based on our observations, we predict that modifying bone remodeling by inhibiting bone resorption may be effective in reducing fibrocartilage degradation in the later but not the earlier stages of TMJ-OA.

BGN and FMOD are members of the small leucine repeat family (SLRP) (6). Members of this family have been shown to regulate collagen fibrillogenesis (24,25), which may explain why in their absence we found a statistically significant increase in the collagen fibril diameters in the condylar cartilage from the 3 month old *Bgn/Fmod* double-deficient mice compared to WT controls. We have previously shown that the WT mice develop TMJ-OA at 18 months (5). In this study, we found that there was an increase in the collagen fibril diameter with age in WT but not in the *Bgn/Fmod* double-deficient mice. Therefore, the increase in the average diameters of the collagen fibrils from both the WT and the *Bgn/Fmod* double-deficient mice appear to be a pre-osteoarthritic biomarker of the condylar cartilage. This theory is supported by similar findings of increased collagen fibril diameters in the cartilage preceding overt osteoarthritis in the knee of mice with a loss-of-function mutation in the gene encoding the alpha1 chain of type XI collagen (26) and in humans with Morquio syndrome (27).

Decreased mechanical strength of the mandibular condylar cartilage may be one of the etiologies behind TMJ-OA in the *Bgn/Fmod* double-deficient mice (28,29). Alterations in the collagen fibril diameters were previously shown to cause decreased mechanical strength of the quadriceps tendons in the *Bgn/Fmod* double-deficient mice (10). Additionally, individual collagen fibril's yield strength has been shown to be inversely proportional to the thickness of the diameter of the collagen fibril (30). However, in the case of mice with the loss of function mutation of the Col XI gene, increased collagen fibril diameters did not initially cause any change in the mechanical properties of the cartilage (26). Therefore, mechanical testing of the mandibular condylar cartilage from the *Bgn/Fmod* double-deficient mice is needed in order to clarify this issue.

In our *Bgn/Fmod* double-deficient mice model, a significant decrease in the expression of *PTHrP* in the mandibular condyle was observed at 3 months before overt TMJ-OA. The decrease in *PTHrP* may be related to TGF-beta growth factor binding and activity. TGF-beta has been shown to induce *PTHrP* expression in murine growth plate cartilages (31) and both BGN and FMOD have been shown to bind to and regulate the activity of members of the TGF-beta family (32). *PTHrP* plays an important role in the propagation and maintenance of mandibular condylar chondrocyte proliferation (33). A decrease in *PTHrP* expression is consistent with our finding of decreased mandibular condylar chondrocyte proliferation in 3 month *Bgn/Fmod* double-deficient mice (5) and may also explain the increase in chondrocyte maturation in the TMJ from 9 month *Bgn/Fmod* double-deficient mice. To clarify the role of *PTHrP* in our mouse model, future studies are planned where *PTHrP* will be injected to condylar cartilage of the 3 month *Bgn/Fmod* double-deficient mice and the progression of TMJ-OA will be monitored.

During overt OA at 9 months in the double-deficient mice, a statistically significant increase in the expression of *Col X* and *Aggrecan* and significant changes in the subchondral bone were

noted. In the subchondral bone a statistically significant decrease in trabecular thickness, and a statistically significant increase in trabecular spacing, trabecular number, total volume, bone volume, and bone surface in the mandibular condylar head was found from the *Bgn/Fmod* double-deficient mice compared to the WT controls. The decrease in trabecular thickness suggests that the increases in bone volume and total volume were not due to increased osteoblast activity. Instead, we believe that the increase in the subchondral volume was due to reactivation of the endochondral maturation pathway. This is further supported by the increase in *Col X*, a marker of hypertrophic chondrocytes. Histological evidence of increased chondrocyte hypertrophy has been reported in a chemical model of TMJ-OA in rabbits (34); however, this is the first report that we are aware of that shows a quantifiable increase in the gene expression of *Col X* in a TMJ-OA model. The increase in chondrocyte maturation seems to be independent of an *Ihh* pathway because there was no significant increase in *Ihh* in 9 month old *Bgn/Fmod* double-deficient mice compared to WT controls. This finding coupled with significant increase in *Aggrecan* and no change in *Sox9* and *Col II* expression, suggest that the increase in chondrocyte maturation was occurring from chondrogenic cells and not from pre-chondrogenic precursors in the mandibular condylar cartilage from the *Bgn/Fmod* double-deficient mice. The observed increase expression of *Aggrecan* and *Col X* has been reported in osteoarthritis of other joints and may be associated with an attempted repair response (12).

From the results of this study, we propose that the absence of BGN and FMOD causes increased collagen fibril diameters and decreased *PTHrP* expression in the condylar cartilage, which preceded overt TMJ-OA and microarchitectural changes in the subchondral bone. These changes may lead to TMJ-OA by decreasing the mechanical strength of the condylar cartilage and/or by the inhibition of growth of the mandibular condylar cartilage. Greater understanding of the early molecular and structural changes during the initial stages of TMJ-OA is critical to the development of targeted therapies to effectively combat the disease process.

Acknowledgments

This work was supported by NIDCR K-22 DE017193 grant and American Association of Orthodontists Foundation Faculty Development Award to SW. This work was also submitted for the partial fulfillment for the requirements for a Master's thesis in the Department of Orthodontics at the University of Connecticut Health Center. We thank Ms. Maya Yankova for assistance in the preparation of samples for electron microscopy.

List of abbreviations

BGN, biglycan; FMOD, fibromodulin; TMJ, temporomandibular joint; OA, osteoarthritis.

REFERENCES

1. Wadhwa S, Kapila S. TMJ disorders: future innovations in diagnostics and therapeutics. J Dent Educ 2008;72(8):930–47. [PubMed: 18676802]
2. Benjamin M, Ralphs JR. Biology of fibrocartilage cells. Int Rev Cytol 2004;233:1–45. [PubMed: 15037361]
3. Shen G, Darendeliler MA. The adaptive remodeling of condylar cartilage---a transition from chondrogenesis to osteogenesis. J Dent Res 2005;84(8):691–9. [PubMed: 16040724]
4. Okenson, J. Management of Temporomandibular Disorders and Occlusion. Vol. Fourth Edition. Mosby, editor. 1998.
5. Wadhwa S, Embree MC, Kilts T, Young MF, Ameye LG. Accelerated osteoarthritis in the temporomandibular joint of biglycan/fibromodulin double-deficient mice. Osteoarthritis Cartilage 2005;13(9):817–27. [PubMed: 16006154]
6. Schaefer L, Iozzo RV. Biological functions of the small leucine-rich proteoglycans: from genetics to signal transduction. J Biol Chem 2008;283(31):21305–9. [PubMed: 18463092]

7. Waddington RJ, Roberts HC, Sugars RV, Schonherr E. Differential roles for small leucine-rich proteoglycans in bone formation. Eur Cell Mater 2003;6:12–21. [PubMed: 14562268]discussion 21
8. Roughley PJ. The structure and function of cartilage proteoglycans. Eur Cell Mater 2006;12:92–101. [PubMed: 17136680]
9. Bi Y, Ehirchiou D, Kilts TM, Inkson CA, Embree MC, Sonoyama W, et al. Identification of tendon stem/progenitor cells and the role of the extracellular matrix in their niche. Nat Med 2007;13(10): 1219–27. [PubMed: 17828274]
10. Ameye L, Aria D, Jepsen K, Oldberg A, Xu T, Young MF. Abnormal collagen fibrils in tendons of biglycan/fibromodulin-deficient mice lead to gait impairment, ectopic ossification, and osteoarthritis. Faseb J 2002;16(7):673–80. [PubMed: 11978731]
11. Ameye LG, Deberg M, Oliveira M, Labasse A, Aeschlimann JM, Henrotin Y. The chemical biomarkers C2C, Coll2-1, and Coll2-1NO2 provide complementary information on type II collagen catabolism in healthy and osteoarthritic mice. Arthritis Rheum 2007;56(10):3336–46. [PubMed: 17907187]
12. Drissi H, Zuscik M, Rosier R, O'Keefe R. Transcriptional regulation of chondrocyte maturation: potential involvement of transcription factors in OA pathogenesis. Mol Aspects Med 2005;26(3): 169–79. [PubMed: 15811433]
13. Kiraly K, Lammi M, Arokoski J, Lapvetelainen T, Tammi M, Helminen H, et al. Safranin O reduces loss of glycosaminoglycans from bovine articular cartilage during histological specimen preparation. Histochem J 1996;28(2):99–107. [PubMed: 8737291]
14. Warshawsky H. A technique for the fixation and decalcification of rat incisors for electron microscopy. Journal of Histochemistry and Cytochemistry 1967;15(9):542–549. [PubMed: 4861607]
15. Sato Y, Imahashi T, Kagimoto A. Electron microscopic observation on a case of sideroblastic anemia. J Electron Microsc (Tokyo) 1967;16(3):283–4. [PubMed: 5594578]
16. Wilda M, Bachner D, Just W, Geerkens C, Kraus P, Vogel W, et al. A comparison of the expression pattern of five genes of the family of small leucine-rich proteoglycans during mouse development. J Bone Miner Res 2000;15(11):2187–96. [PubMed: 11092399]
17. Xu T, Bianco P, Fisher LW, Longenecker G, Smith E, Goldstein S, et al. Targeted disruption of the biglycan gene leads to an osteoporosis-like phenotype in mice. Nat Genet 1998;20(1):78–82. [PubMed: 9731537]
18. Gill MR, Oldberg A, Reinholt FP. Fibromodulin-null murine knee joints display increased incidences of osteoarthritis and alterations in tissue biochemistry. Osteoarthritis Cartilage 2002;10(10):751–7. [PubMed: 12359160]
19. Silbermann M, Livne E. Age-related degenerative changes in the mouse mandibular joint. J Anat 1979;129(Pt 3):507–20. [PubMed: 541239]
20. Ameye LG, Young MF. Animal models of osteoarthritis: lessons learned while seeking the "Holy Grail". Curr Opin Rheumatol 2006;18(5):537–47. [PubMed: 16896297]
21. Dieppe P, Cushnaghan J, Young P, Kirwan J. Prediction of the progression of joint space narrowing in osteoarthritis of the knee by bone scintigraphy. Ann Rheum Dis 1993;52(8):557–63. [PubMed: 8215615]
22. Garnero P, Aronstein WS, Cohen SB, Conaghan PG, Cline GA, Christiansen C, et al. Relationships between biochemical markers of bone and cartilage degradation with radiological progression in patients with knee osteoarthritis receiving risedronate: the Knee Osteoarthritis Structural Arthritis randomized clinical trial. Osteoarthritis Cartilage 2008;16(6):660–6. [PubMed: 17993283]
23. Bingham CO 3rd, Buckland-Wright JC, Garnero P, Cohen SB, Dougados M, Adami S, et al. Risedronate decreases biochemical markers of cartilage degradation but does not decrease symptoms or slow radiographic progression in patients with medial compartment osteoarthritis of the knee: results of the two-year multinational knee osteoarthritis structural arthritis study. Arthritis Rheum 2006;54(11):3494–507. [PubMed: 17075851]
24. McEwan PA, Scott PG, Bishop PN, Bella J. Structural correlations in the family of small leucine-rich repeat proteins and proteoglycans. J Struct Biol 2006;155(2):294–305. [PubMed: 16884925]
25. Vogel KG, Trotter JA. The effect of proteoglycans on the morphology of collagen fibrils formed in vitro. Coll Relat Res 1987;7(2):105–14. [PubMed: 3621881]

26. Xu L, Flahiff CM, Waldman BA, Wu D, Olsen BR, Setton LA, et al. Osteoarthritis-like changes and decreased mechanical function of articular cartilage in the joints of mice with the chondrodysplasia gene (cho). Arthritis Rheum 2003;48(9):2509–18. [PubMed: 13130470]
27. Bank RA, Groener JE, van Gemund JJ, Maaswinkel PD, Hoeben KA, Schut HA, et al. Deficiency in N-acetylgalactosamine-6-sulfate sulfatase results in collagen perturbations in cartilage of Morquio syndrome A patients. Mol Genet Metab 2009;97(3):196–201. [PubMed: 19394256]
28. Hsieh CH, Lin YH, Lin S, Tsai-Wu JJ, Wu CH Herbert, Jiang CC. Surface ultrastructure and mechanical property of human chondrocyte revealed by atomic force microscopy. Osteoarthritis Cartilage 2008;16(4):480–8. [PubMed: 17869545]
29. Temple MM, Bae WC, Chen MQ, Lotz M, Amiel D, Coutts RD, et al. Age- and site-associated biomechanical weakening of human articular cartilage of the femoral condyle. Osteoarthritis Cartilage 2007;15(9):1042–52. [PubMed: 17468016]
30. Shen ZL, Dodge MR, Kahn H, Ballarini R, Eppell SJ. Stress-strain experiments on individual collagen fibrils. Biophys J 2008;95(8):3956–63. [PubMed: 18641067]
31. Serra R, Karaplis A, Sohn P. Parathyroid hormone-related peptide (PTHrP)-dependent and -independent effects of transforming growth factor beta (TGF-beta) on endochondral bone formation. J Cell Biol 1999;145(4):783–94. [PubMed: 10330406]
32. Hildebrand A, Romaris M, Rasmussen LM, Heinegard D, Twardzik DR, Border WA, et al. Interaction of the small interstitial proteoglycans biglycan, decorin and fibromodulin with transforming growth factor beta. Biochem J 1994;302(Pt 2):527–34. [PubMed: 8093006]
33. Shibukawa Y, Young B, Wu C, Yamada S, Long F, Pacifici M, et al. Temporomandibular joint formation and condyle growth require Indian hedgehog signaling. Dev Dyn 2007;236(2):426–34. [PubMed: 17191253]
34. Cledes G, Felizardo R, Foucart JM, Carpentier P. Validation of a chemical osteoarthritis model in rabbit temporomandibular joint: a compliment to biomechanical models. Int J Oral Maxillofac Surg 2006;35(11):1026–33. [PubMed: 16829037]

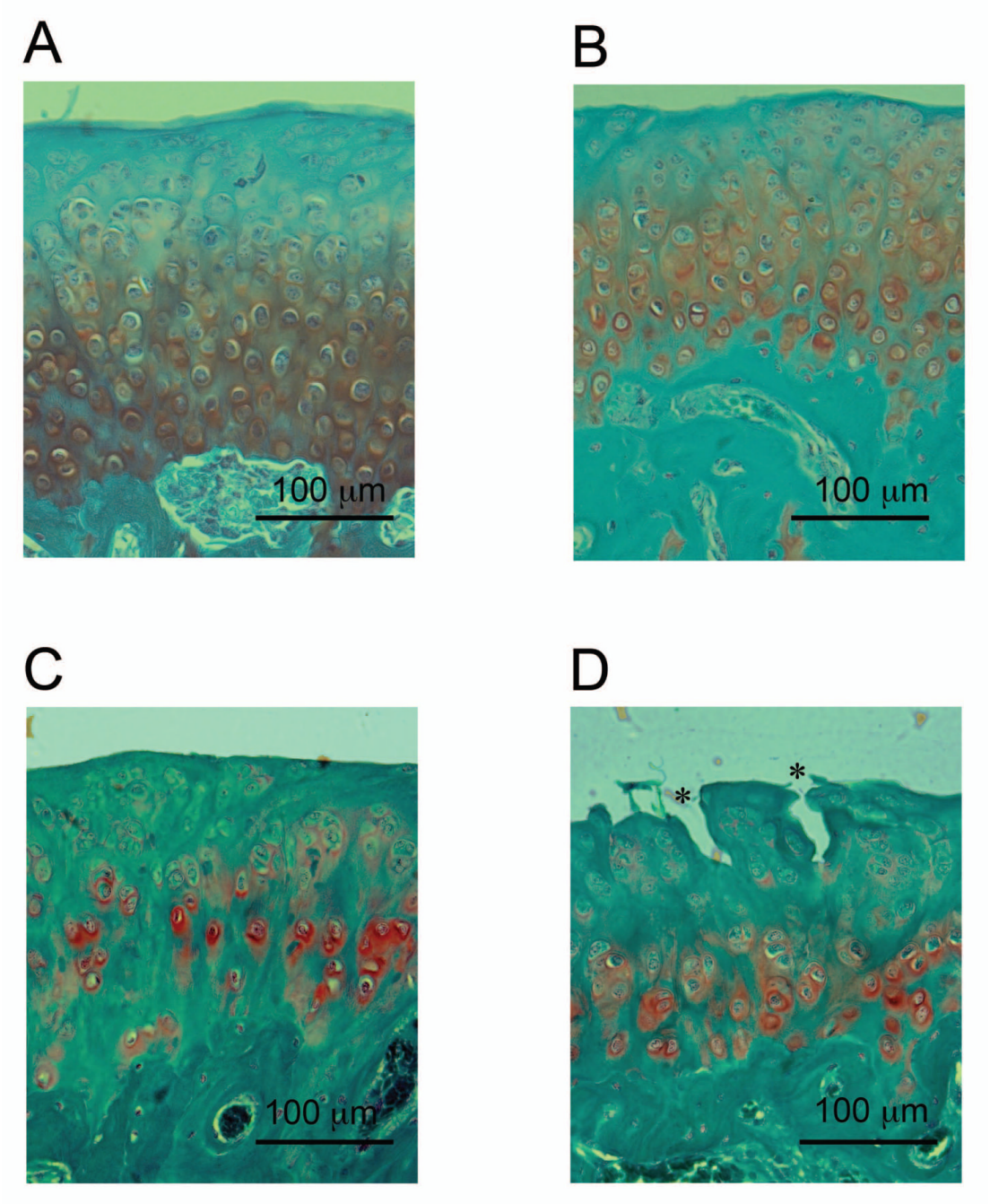

Figure 1.

Representatives of the Safranin O staining (red) of the condylar cartilage. Sections were counter stained with Fast Green. (A) 3 month WT; (B) 3 month *Bgn/Fmod* double-deficient; (C) 9 month WT; and (D) 9 month *Bgn/Fmod* double-deficient. Asterisks (*) represent vertical clefts which form in the mandibular condylar cartilage from 9 month *Bgn/Fmod* double-deficient mice. WT = wild-type; *Bgn* = biglycan; and *Fmod* = fibromodulin.

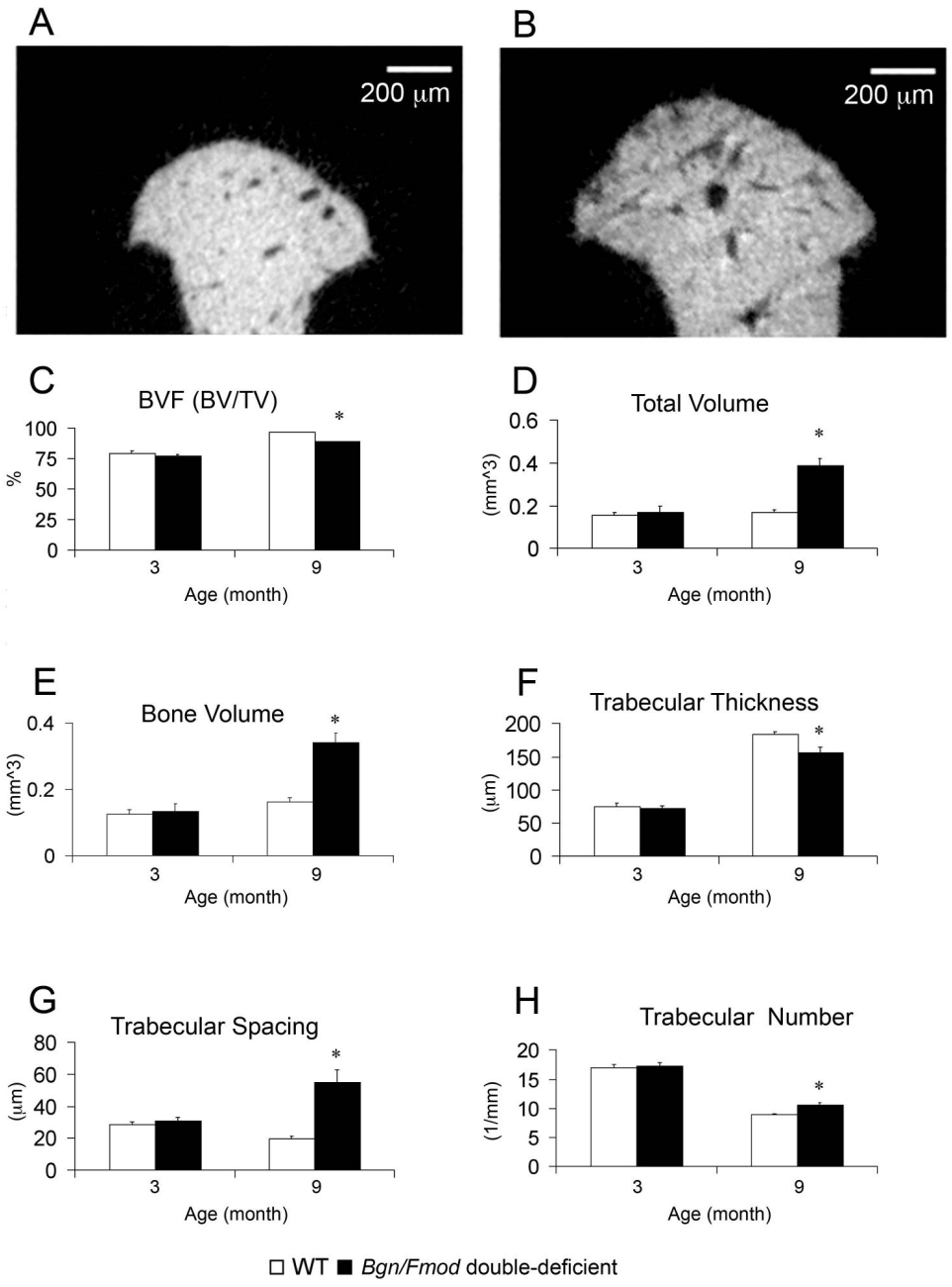

Figure 2.

Micro-CT analysis of the subchondral bone. Representative images of midsagittal cross sections from the mandibular condylar head of a 9 month WT mouse (A) and a 9 month *Bgn/Fmod* double-deficient mouse (B). Analysis of bone volume fraction (C), total volume (D), bone volume (E), trabecular thickness (F), trabecular spacing (G), and trabecular number (H) from the mandibular condylar subchondral bone of a total of 24 mice. Analysis was conducted at two time points: 3 months, WT (n = 6) and *Bgn/Fmod* double-deficient (n = 5), and 9 months, WT (n = 6) and *Bgn/Fmod* double-deficient (n = 7). Asterisk (*) denotes a statistically significant difference between WT and *Bgn/Fmod* double-deficient mice ($p < 0.05$). WT = wild-type; *Bgn* = biglycan; and *Fmod* = fibromodulin.

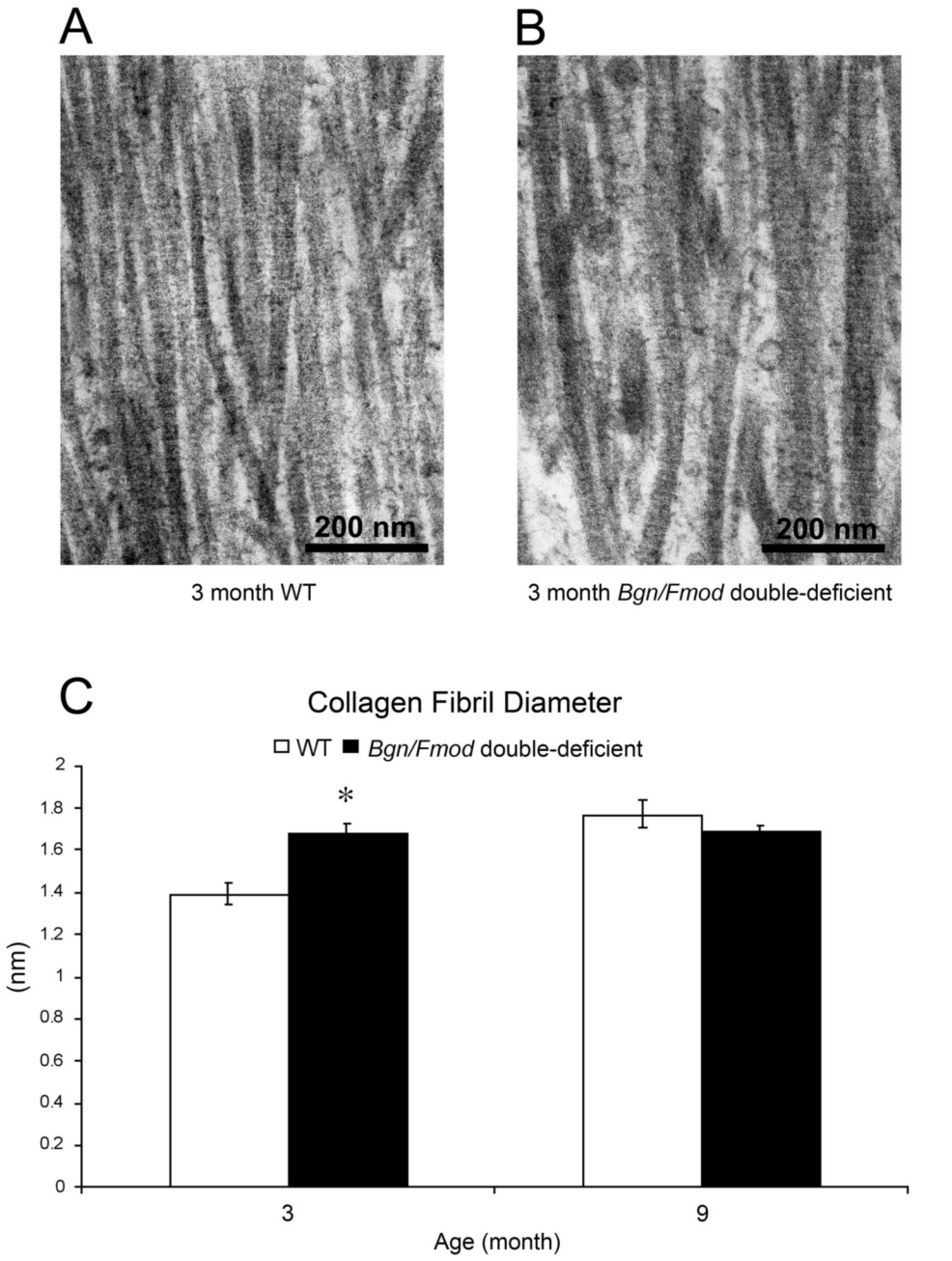

Figure 3.

Transmission Electron Microscopy (TEM) analysis of the condylar cartilage. TEM images of (A) 3 month WT and (B) 3 month *Bgn/Fmod* double-deficient mice. (C) A graphic representation of the data comparing 3 month WT and *Bgn/Fmod* double-deficient mice versus the 9 month WT and *Bgn/Fmod* double-deficient mice. Analysis was conducted at two time points for a total of 26 mice: 3 months, WT (n = 6) and *Bgn/Fmod* double-deficient (n = 6), and 9 months, WT (n = 6) and *Bgn/Fmod* double-deficient (n = 8). Asterisk (*) denotes a statistically significant difference between WT and *Bgn/Fmod* double-deficient mice ($p < 0.05$). WT = wild-type; *Bgn* = biglycan; and *Fmod* = fibromodulin.

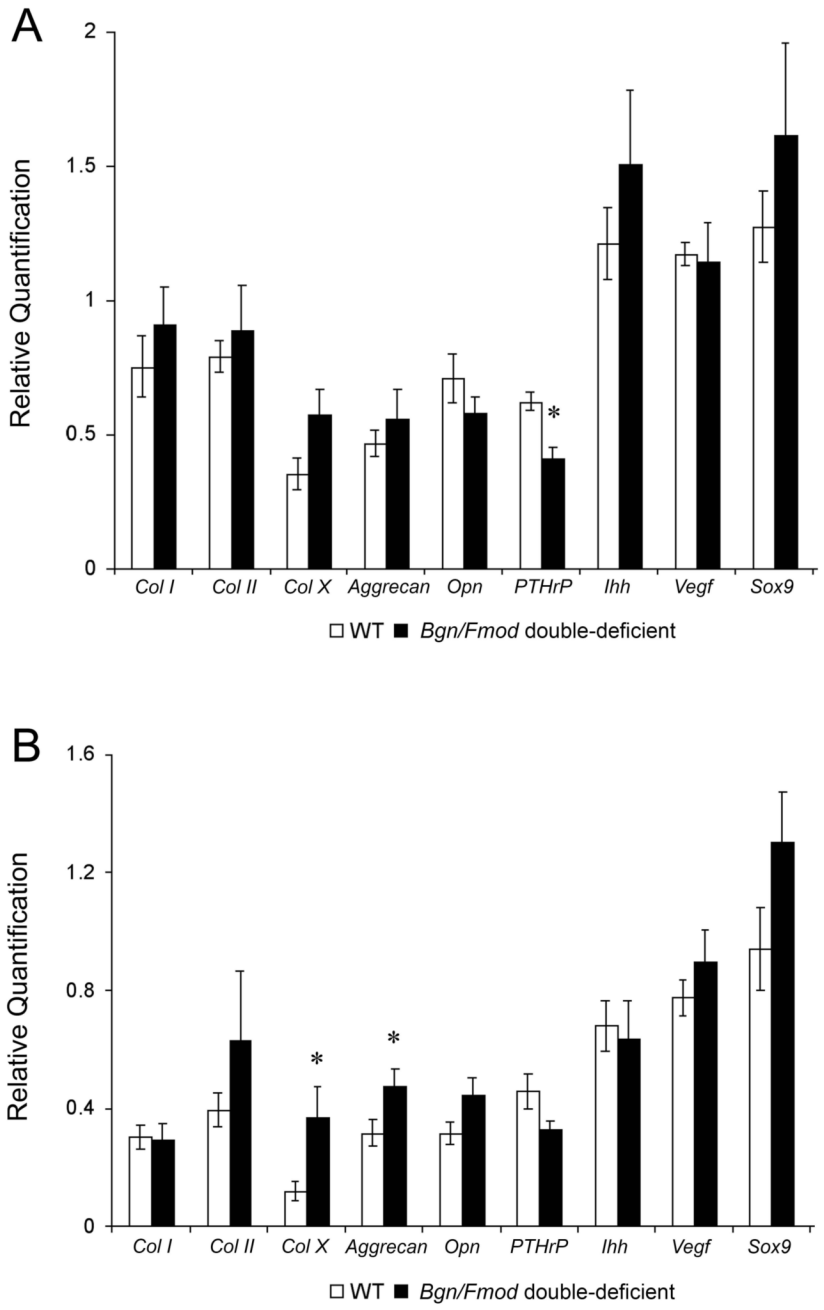

Figure 4.

Real time PCR analysis for Parathyroid hormone related protein (*PTHrP*), SRY-box containing gene 9 (*Sox9*), Collagen type II (*Col II*), Indian hedgehog (*Ihh*), Collagen type X (*Col X*), Vascular endothelial growth factor (*Vegf*), Osteopontin (*Opn*), Collagen type 1 (*Col I*), and *Aggrecan* gene expression from the mandibular condylar head from 3 month WT and *Bgn/Fmod* double-deficient mice (A), and 9 month WT and *Bgn/Fmod* double-deficient mice (B). Analysis was conducted at two time points for a total of 45 mice: 3 months, WT (n = 10) and *Bgn/Fmod* double-deficient (n = 10), and 9 months, WT (n = 13) and *Bgn/Fmod* double-deficient (n = 12). Asterisk (*) denotes a statistically significant difference between WT and

Bgn/Fmod double-deficient ($p < 0.05$) mice. WT = wild-type; *Bgn* = biglycan; and *Fmod* = fibromodulin.